# Memo on the Development and Availability of Dynamically Downscaled Projections Using WRF

Prepared by Stefan Rahimi, UCLA
April, 2022


- This research is funded by the California Energy Commission (CEC) through its Electric Program Investment Charge (EPIC) Program, which invests in scientific and technological research to accelerate the transformation of the electricity sector to meet the state's energy and climate goals.

- The research project, EPC-20-006, will integrate the latest downscaling approaches applied to the recently produced global climate models (GCMs) with an engagement process to develop a robust, usable, set of climate projections applicable for California.
- This memo and data here within are being shared to support transparent and timely consideration of interim deliverables that are relevant for energy stakeholders and all those interested in California's next generation of climate projections. The memo does include data that was part of non-CEC leveraged projects.

This memorandum is submitted to the CEC by UC San Diego's Scripps Institution of Oceanography. The report meets deliverable requirements under Task 4 of the California Energy Commission's Project EPC-20-006: Development of Climate Projections for California and Identification of Priority Projections.

## Synopsis

This document describes a new suite of dynamically downscaled climate-scale data delivered to CEC under award EPC-20-006, "Development of Climate Projections for California and Identification of Priority Projections", Task 4, as part of a broader downscaling effort. Specifically, select global climate model (GCM) projections from the 6th coupled model intercomparison project (CMIP6) are physically transformed to high spatial resolutions from 1980 through 2100 by a regional climate model. The results from the dynamically downscaled projections will contain spatial patterns of climate that evolve throughout the 21st century, including changes in this dynamic system, that will be used as training for LOCA, a statistical downscaling approach (Task 5). A historical reanalysis is also dynamically downscaled from 1950-2021. The memorandum describes dynamical downscaling and then provides information about the synthesis and structure of the dynamically downscaled projections and reanalysis. A similar method that is described here will be employed for targeted case studies (Task 8) that will be available later in the project. While the focus is mainly on the dynamically downscaled reanalysis and 4 GCMs, we also touch on the other GCMs that have been downscaled via leveraged projects and may be of interest to the energy sector and beyond.

## 1. Introduction

GCMs are the primary tool by which future climate projections are created; however, they do not have sufficiently small grid spacing to allow for facility-level and watershed-specific forecasts. Thus, some type of technique must be used to synthesize plausible future projections that capture local geographic complexities that may drive local weather, hydrology, and climate (e.g., mountains, coastlines, lakes, etc.). The term 'downscaling' generally describes this synthesis process, and its etymology is tied to the concept that in nature, energy in the atmosphere tends to be transferred from larger processes or systems to smaller processes or systems. An example of this is a landfalling atmospheric river (AR); its kinetic energy (i.e., winds) originates from large-scale horizontal temperature differences and the earth's rotation. The smaller-scale precipitation segments associated with the AR derive their energy from the parent storm system and serve as a conduit by which energy is passed on to even smaller scales of motion, driving processes such as turbulence, as the overall system attempts to distribute energy equally, everywhere. Downscaling of GCMs is the term used to describe the umbrella of techniques by which smaller-scale weather, hydrologic, and climate features can be estimated by using physics and statistics.

For dynamical downscaling, a mere seven laws of nature are used by a regional climate model (RCM) to arrive at the desired high-resolution end-product. Specifically, the RCM 'ingests' the GCM-simulated temperature, horizontal winds, moisture content, sea surface temperatures, soil properties, and atmospheric pressure fields at sub-daily time intervals, integrating a high-resolution solution across a limited area of the planet. The ingested GCM information serves to constrain the RCM solution, which itself contains high-resolution topography and other geo-features needed to simulate a more spatially heterogeneous future across a given area.

Broad applications of dynamical downscaling across large GCM ensembles are hampered by computational resource limitations, and GCM data availability.  From a computational standpoint, each of our GCM simulations require the equivalent of nearly 26,000 personal computers run continuously and simultaneously for almost 9-days without pause; this amounts to a very expensive computational endeavor. Regarding GCM data availability, only a subset of CMIP6 GCMs have saved the 3-dimensional atmospheric drivers having sufficient temporal resolution, sufficiently-high vertical resolution, and proper model initialization needed by a regional atmospheric model for dynamical downscaling. Furthermore, only a portion of the CMIP6 GCMs grade out as sufficiently skillful in reproducing observed atmospheric processes and regional weather and climate variability.

Amongst a growing set of dynamical downscaling-capable RCMs, the Weather Research and Forecasting (WRF) model is one of the most widely maintained and used RCMs for research and operational applications, and it has a superior customizability compared to other RCMs in terms of selecting its physical parameters and solvers. Thus, we were able to select a physical configuration of the model tailor-made for simulating western US weather and climate (briefly described in 2.1.1 and in Rahimi et al., 2022). Our compliance with best practices in WRF effectively limits the number of GCM simulation candidates from thousands (accounting ~35 GCMs from international modeling centers, different emissions pathways, and multiple ensemble members of each) to a mere ~150. We add that, of these 150 GCM simulations, only 13 are relatively independent of one another in terms of their physical solvers, parameterizations, and dynamic cores (variations of the 7 fundamental physical laws).

Lastly, the plethora of available RCMs use different physical solvers and dynamic cores to downscale the GCMs which can introduce uncertainty. For instance, a RCM may have a default convective scheme better suited for tropical climates that may not be as apt for modeling in the midlatitudes. Thus, its solution may differ from that of another RCM which uses a more generalized convective scheme; choosing the best RCM and options within is a nontrivial process. The ability of RCMs to represent regional weather differently adds to uncertainty in the finalized downscaled result, and the aforementioned GCM data requirements prevent dynamically downscaling from being applied to a greater number of GCMs simulations. Nonetheless, dynamical downscaling provides physically-derived continuous weather and climate evolution information which is extremely valuable in assessing future weather extremes and climate.

# 2. Development of Model Set up for Dynamical Downscaling

All testing and production of the dynamical downscaled data were conducted on the NCAR-Wyoming Cheyenne supercomputing cluster. Although Dr. Rahimi secured the compute resources to complete the experiments, we also acknowledge the generous support of Dr. Zachary Lebo at the University of Wyoming via the UCAR Computational Information Systems Lab (see supporting letter in proposal documents).

## 2.1 Conducting the simulations

### 2.1.1 Testing and reanalysis-driven experiments

The RCM used in dynamical downscaling is the WRF model version 4.1.3. With our prime goal being to dynamically downscale CMIP6 GCMs, the general decision was made to dynamically downscale GCM forcing datasets to a 45-km grid first and use that simulations output to drive an inner 9-km simulations (see grids in Fig. 1a) via one-way nesting, meaning the larger grid only pushed the data to the smaller high-resolution grid. Finally, two 3-km experiments (one over California and one over Wyoming) were driven using the 9-km simulation outputs. The California nest supports EPC-20-006 and the Wyoming nest supports another project that provided the computing resources. WRF simulations are carried out on 39 vertical levels, with a varying vertical grid spacing on the order of 100 meters in the boundary layer and stretching to hundreds to a few thousands of meters higher up. This ‘stretching’ of the vertical grid allows for features in the lower troposphere, which are characterized by fine vertical variations than those aloft, to be better simulated while meteorological features in the middle and upper troposphere with smaller vertical variations are still sufficiently resolved.

WRF is an extremely sophisticated but complex RCM (Skamarock et al., 2019), containing tens of thousands of combinations of base physical solver packages wrapped up in 3-4 million lines of code. To identify a preferred set of physical solver options for downscaling with WRF across the western US and California, we conducted 21 year-long tests in which either the North American Regional Reanalysis (Mesinger et al., 2006) or the European Center for Medium-range Weather Forecasting's 5th Reanalysis (ERA5) (Hersbach et al., 2020) were downscaled for water year 2010 (described in Rahimi et al., 2022) onto the grids shown in Fig. 1a, and tests prioritized the 9-km and 3-km grids. We began by identifying a base set of solvers commonly used in other published studies across the region. As solvers were updated throughout testing, general reductions in precipitation, snow, wind, and to a lesser degree streamflow biases were noted at weather (SNOTEL and METAR) and hydrologic (GAGES-II) stations in Fig. 1b, especially with increasing horizontal resolution (smaller grid spacings). ERA5-driven tests generally outperformed NARR-driven tests. The superior performance in ERA5-driven tests, coupled with its longer historical scope (1950 onwards) compared to NARR, motivated us to choose ERA5 as our forcing reanalysis.

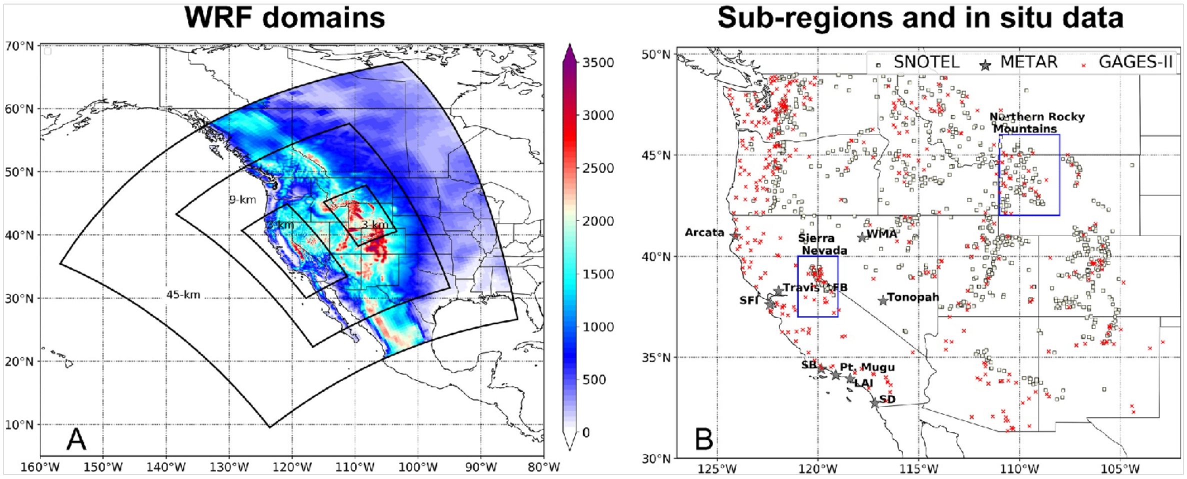


*Figure 1. (a) WRF domain coverage for the 45-km, 9-km, and 3-km experiments. The filled color contours represent the terrain height [m] in the highest-resolution domain that covers the given pixel. presents the two subregions that we consider in our targeted evaluations (blue outline), specifically the Sierra Nevada (SN) and the Northern Rocky Mountains (NRMs), as well as in situ SNOTEL (squares), METAR (stars), and GAGES-II (red crosshatches) data locations used in WRF performance evaluations.*

Our test results informed a subsequent downscaling effort in which ERA5 was dynamically downscaled from 1 August 1950 through 1 September 2021, on the same grids shown in 1a. To simulate a 70-year period in a reasonable real-world time frame, we chose to simulate each fiscal year, defined from 1 August through 1 September of the following year (13 months), simultaneously and in parallel, independent of each other, from 1950-2021, discarding the first month of these discrete 13-month simulations as spin-up. The spin-up period is nominally designed to allow WRF's simulated soil properties to reach an equilibrium state, although it should be noted that spin-up periods of a year or more are desired in hydrologic modeling. Nonetheless, we then reconstructed the full time series by stitching together the remaining data in chronological order. We note that, without this parallelization approach, the time to complete the ERA5 simulation would be increased from roughly 9 days to 1 year. Each fiscal year was initialized to the ERA5 state, and spectral nudging of the large-scale meteorological patterns was implemented to prevent WRF from drifting too far from the forcing reanalysis state; features with spatial wavelengths of ~1,500 km or larger are preserved in downscaling, while WRF integrated its own internal higher-resolution meteorological features.

The downscaled ERA5 product provides a useful baseline historical dataset by which to compare downscaled GCMs across the western US and California over climate time scales. As can be seen in Rahimi et al., 2022, however, this dataset is characterized by biases that must be acknowledged by end-users including (i) a high-elevation wet bias on the order of 5%, (ii) a summertime wet bias across the desert southwest of less than 1 mm day$^{-1}$ (but can be ~100%), and finally a low (high) elevation warm (cold) temperature bias that can be as large as a few Kelvin in magnitude on seasonal time scales. Biases in a subset of widely-used surface variables will mostly be removed from the dataset by the LOCA team's bias correction procedure (part of Task 5), which is not discussed here.

### 2.1.2 GCM simulations

In addition to the ERA5-driven WRF simulation, we dynamically downscale four CMIP6 GCMs from 1980-2100 using the same yearly discretization approach and the same set of physics solvers configured in WRF. We only downscale four GCMs to 3 km due to the high computational costs involved in the dynamical downscaling process of even a single GCM. Limited compute resources, in addition to the more than 30 GCMs reporting to CMIP6, each potentially containing multiple future emissions scenarios and realizations, facilitates a need for a GCM screening process described below.

Here, we dynamically downscale GCMs subject to the following requirements:

1. GCM-simulated atmospheric data are available at sub-daily time intervals as we seek to resolve the synoptic-scale evolution of weather patterns from the parent simulation. Specifically, 4 sub-daily fields are required, and we require a total of 8 (preferably daily) state/kinematic variables from the land surface and atmosphere for WRF to yield physical results. If any of these variables are absent, we cannot effectively downscale the GCM.
2. The GCM must exhibit acceptable performance in simulating the observed northern hemispheric circulation patterns, Pacific Ocean oceanic conditions, and other atmospheric properties characteristic of eastern Pacific Basin/western North American climate relative to other CMIP6 GCMs over the historical period. The evaluation process is described below.
3. After determining a GCM shortlist in (2), we further refine potential GCMs based on their linear independence from each other, as some GCMs share the same code bases.
4. Finally, we select our GCMs based on the spread in their respective future climate change signals. For instance, two of our selected GCMs described below have wetter futures across California while the other two have a neutral or drier future across California

As discussed above, models are selected for downscaling by a multi-step evaluation process that prioritizes both the skill of models over the Western US and the balanced representation of future climate scenarios. The skill of models is evaluated by comparison to ERA5 reanalysis data in the historical period through two sets of metrics. The first set evaluates model performance on temperature and precipitation over several timescales within the downscaling domain. The second set evaluates larger-scale patterns of circulation and variability across the northern hemisphere that are particularly important for creating realistic boundary conditions for the regional model. Models that perform well across both sets of metrics are prioritized for downscaling. Within the available realizations of the top performing models, the final set for downscaling is selected to achieve a balance of model diversity, a representative range of overall change to temperature and precipitation, and a set of storylines that capture significant climate events such as droughts and heatwaves that are helpful for regional adaptation planning. More information on the GCM selection process can be found in the *Evaluation of CMIP6 GCMs Relevant for California Report* by W. Kranz et al. (Task 3) submitted to the CEC.

Based the GCM selection process described above, the dynamically downscaled GCMs for CEC are:

1. CESM2 r11i1p1f1
    a. historical from 1980-2014
    b. SSP3-7.0 from 2015-2100
    c. 45 km, 9km, and 3 km domain
2. CNRM-ESM2-1 r1i1p1f2
    a. historical from 1980-2014
    b. SSP3-7.0 from 2015-2100
    c. 45 km, 9km, and 3 km domain
3. EC-Earth3-Veg r1i1p1f1
    a. historical from 1980-2014
    b. SSP3-7.0 from 2015-2100
    c. 45 km, 9km, and 3 km domain
4. FGOALS-g3 r1i1p1f1
    a. historical from 1980-2014
    b. SSP3-7.0 from 2015-2100
    c. 45 km, 9km, and 3 km domain

**Please note: No pre-downscaling bias correction is applied to any of these 4 WRF-downscaled GCM simulations.**

Figure 2 depicts future changes in cumulative annual water year precipitation from our 4 GCMs (top row of images) and their dynamically downscaled counterparts (bottom row of images).

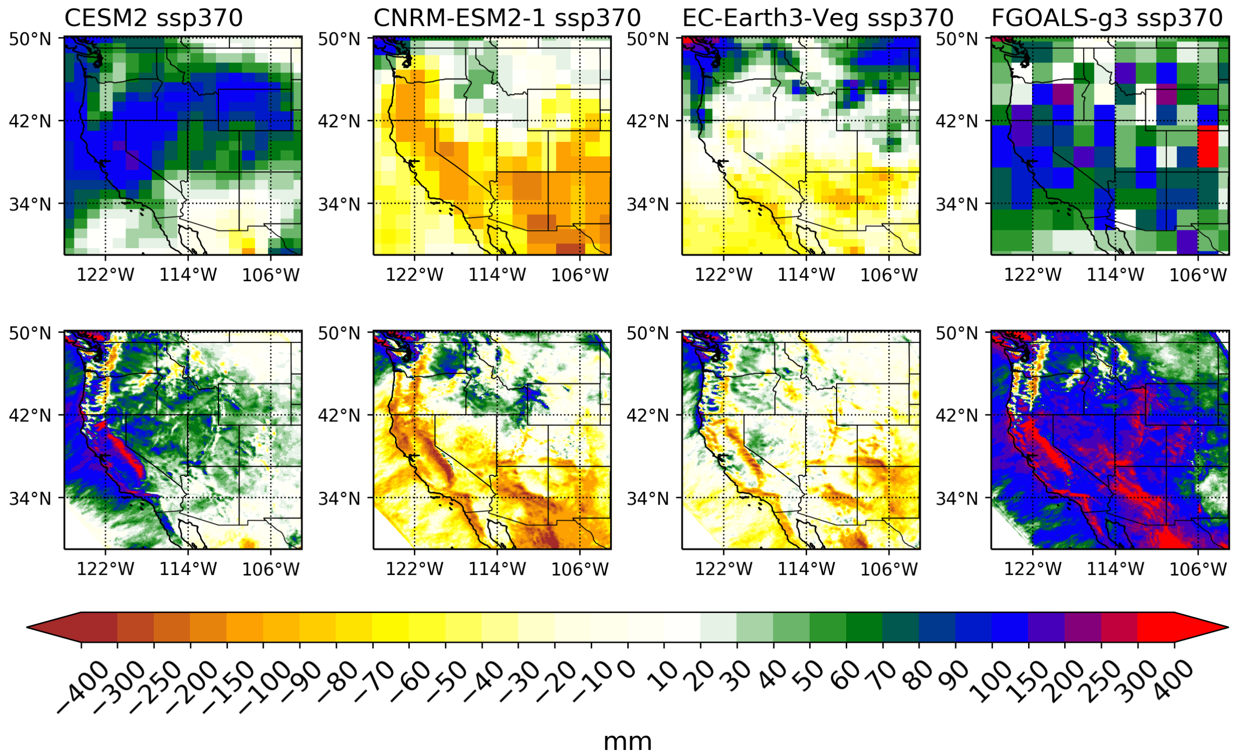


*Figure 2. Future (2070-2100 mean) minus present-day (1980-2010 mean) differences in cumulative annual water year precipitation in [mm] for the four WRF-downscaled GCMs. The top row shows the climate change signal from the native GCMs while the bottom row shows the same but on the dynamically downscaled 9-km grid. Note that the WRF solution generally preserves the large-scale characteristics of the parent GCM.*

CMIP6 historical GCM output is used to drive WRF from 1 August 1980 through 31 December 2014, while CMIP6 ScenarioMIP GCM output is used to drive WRF from 1 January 2015 through 1 September 2100. Anthropogenic emissions from the third Shared Socioeconomic Pathway (SSP3) with an end-century top-of-the-atmosphere radiative forcing of 7 W $m^{-2}$ is (SSP3-7.0) are used beyond 2014. We chose SSP3-7.0 as our future emissions scenario because its future change has a large signal-to-noise ratio and because it is increasingly unlikely that the maximum emissions scenario (SSP5-8.5) will be realized due to increasing international mitigation efforts. We note that the LOCA Hybrid downscaling (Task 5) will include a much larger suite of models and three different SSPs.

As a part of UCLA's participation in NCAR's Advanced Scientific Discovery program on their new supercomputer, Derecho, 15-20 additional GCMs are to be dynamically downscaled by the end of 2022. That downscaling will use the same WRF methods as discussed above and will also be made available to the IOUs, as well as the energy and climate community. The additional GCM simulations that will be dynamically downscaled will be primarily based on the requirements of the Advanced Scientific Discovery Program, which awarded the supercomputing time enabling the dynamically downscaling of additional simulations. However, the additional dynamically downscaled GCM simulations also benefit EPC-20-006 and thus, we will use the GCMs selection process described above and the input from stakeholders, particularly feedback from the Working Group meeting on Feb 4th focused on model selection, as possible to determine which models will be additionally downscaled.

For the CEC, the variables listed below are provided on the 45-, 9-, and 3-km California WRF grid. Please note that for other tasks within EPC-20-006 the WRF results will be used in different ways by the LOCA and hydrologic modeling teams. We emphasize that dynamically downscaled data as part of this Task 4 and presented below are not bias corrected in any way following downscaling**.** As WRF testing and early model runs leveraged other projects, the initial set of variables were chosen based on feedback from hydrologic, fire, and land-surface modelers and researchers. We evaluated the variables against the *Synthesis of Variables, Spatial and Temporal Scales required from all use-cases*, which was shared in the EPC-20-006 2021 Quarter 4 progress report. An important variable identified from the use cases was wind gusts, however, maximum hourly wind gusts could not be saved as it would have increased our computational costs by 20% and thus could not be accommodated.

Below are the 21 **hourly** variables we provide.

| **Name** | **Units** |
|---|---|
| 1. 2-m temperature | [K] |
| 2. 2-m specific humidity | [kg kg-1] |
| 3. Surface pressure | [Pa] |
| 4. 10-m u-component of the wind (grid relative) | [m s-1] |
| 5. 10-m v-component of the wind (grid relative) | [m s-1] |
| 6. Snow water equivalent | [mm] |
| 7. Skin temperature | [K] |
| 8. Non-convective precipitation (cumulative) | [mm] |
| 9. Convective precipitation (cumulative) | [mm] |
| 10. Cumulative snowfall equivalent | [mm] |
| 11. Diffuse downwelled solar radiation | [W m-2] |
| 12. Surface upwelled solar radiation (all sky) | [W m-2] |
| 13. Surface upwelled solar radiation (clear sky) | [W m-2] |
| 14. Surface downwelled solar radiation (all sky) | [W m-2] |
| 15. Surface downwelled solar radiation (clear sky) | [W m-2] |
| 16. Surface upwelled longwave radiation (all sky) | [W m-2] |
| 17. Surface upwelled longwave radiation (clear sky) | [W m-2] |
| 18. Surface downwelled longwave radiation (all sky) | [W m-2] |
| 19. Surface downwelled longwave radiation (clear sky) | [W m-2] |
| 20. Surface runoff | [mm s-1] |
| 21. Sub-surface runoff | [mm s-1] |

As with the hourly outputs, we provide 37 variables post-processed **daily** time scales. Noting that convective precipitation is only nonzero in the 45- and 9-km simulations, we provide:

| Name | Units | Label |
|---|---|---|
| 1. 2-m average temperature | [K] | 't2' |
| 2. 2-m minimum temperature | [K] | 't2min |
| 3. 2-m maximum temperature | [K] | 't2max' |
| 4. Maximum hourly precipitation | [mm h-1] | 'prec_max' |
| 5. 2-m specific humidity | [kg kg-1] | 'q2' |
| 6. Maximum 10-m wind speed | [m s-1] | 'wspd10max' |
| 7. Snow water equivalent | [mm] | 'snow' |
| 8. Precipitation rate | [mm d-1] | 'prec' |
| 9. Snow precipitation rate | [mm d-1] | 'prec_snow' |
| 10. Relative humidity | [0-100] | 'rh' |
| 11. Integrated vapor transport (zonal and meridional components; earth relative) | [kg s-1 m-1] | 'ivt' |
| 12. Ice water path | [kg m-2] | 'iwp' |
| 13. Liquid water path | [kg m-2] | 'lwp' |
| 14. Soil moisture | [m3 m-3] | 'soil_m' |
| 15. Soil temperature | [K] | 'soil_t' |
| 16. Skin temperature | [K] | 'tskin' |
| 17. Surface pressure | [Pa] | 'psl' |
| 18. Surface runoff | [mm d-1] | 'sfc_runoff' |
| 19. Sub-surface runoff | [mm d-1] | 'subsfc_runoff' |
| 20. Evaporation | [mm d-1] | 'evap_sfc' |
| 21. Evapotranspiration | [mm d-1] | 'etrans_sfc' |
| 22. Downwelled SW at surface (> 0 into sfc) | [W m-2] | 'sw_dwn' |
| 23. Downwelled LW at surface (> 0 into sfc) | [W m-2] | 'lw_dwn' |
| 24. Net SW flux at the surface (> 0 into sfc) | [W m-2] | 'sfc_sfc' |
| 25. Net LW flux at surface (> 0 into atm) | [W m-2] | 'lw_sfc' |
| 26. Sensible heat flux at surface (> 0 into atn) | [W m-2] | 'sh_sfc' |
| 27. Latent heat flux at surface (> 0 into atm) | [W m-2] | 'lh_sfc' |
| 28. Ground heat flux at surface (> into atm) | [W m-2] | 'gh_sfc' |
| 29. 3-D q | [kg kg-1] | 'q_3d |
| 30. 3-D w | [m s-1] | 'w_3d |
| 31. 10-m u, v (earth relative) | [m s-1] | 'uv10' |
| 32. 3-D u (earth relative) | [m s-1] | 'u_3d' |
| 33. 3-D v (earth relative) | [m s-1] | 'v_3d' |
| 34. 3-D geopotential height | [m2 s-2] | 'phi_3d' |

| | | |
|---|---|---|
| 35. 3-D temperature | [K] | ‘t_3d’ |
| 36. Convective precipitation | [mm d-1] | ‘prec_c’ |
| 37. Mean 10-m wind speed | [m s-1] | ‘wspd10mean’ |

The full 6-hourly WRF datastream for all grids (45-, 9-, and 3-km) in its native output form can be found in the Amazon S3 bucket described in the data access section below. The best way to examine the file contents is by loading a 6-hourly file into memory and examining the data keys. More than 200 variables are provided in each 6-hourly file.

In addition to the four dynamically downscaled GCMs for the CEC mentioned above, in our data catalog (https://dept.atmos.ucla.edu/alexhall/downscaling-cmip6), there are additional GCM downscaled simulations. These simulations are a combination of our larger research effort to better understand and test methods that are used to dynamically downscaling GCMs. Some of the runs were conducted prior to the start of this project and others were conducted to address other research projects’ objectives. Specifically, we were examining the effects of pre-dynamically downscaling (a priori) bias correction. As a result, several of these experiments are simply variations of four aforementioned GCMs in which a pre-downscaling bias correction of the mean-state was applied following Bruyère et al., 2014.This is discussed more below in Section 4. Simulations in this category were generally downscaled to 9-km with the exception of EC-Earth3-Veg. The variables for these simulations are the same as is listed above. As of 29 March 2022, the following GCMs have also been dynamically downscaled:

1. CESM2 r11i1p1f1 for SSP2-4.5 down to 9-km
    a. historical from 1980-2014
    b. SSP2-4.5 from 2015-2100
2. CESM2 r11i1p1f1 for SSP5-8.5 down to 9-km
    a. historical from 1980-2014
    b. SSP5-8.5 from 2015-2100
3. CESM2 r11i1p1f1 for SSP3-7.0 with pre-downscaling bias correction down to 9-km
    a. historical from 1980-2014
    b. SSP3-7.0 from 2015-2100
4. MPI-ESM1-2-LR for SSP3-7.0 down to 9-km
    a. historical from 1980-2014
    b. SSP3-7.0 from 2015-2100
5. MPI-ESM1-2-LR for SSP3-7.0 with pre-downscaling bias correction down to 9-km
    a. historical from 1980-2014
    b. SSP3-7.0 from 2015-2100
6. CNRM-ESM2-1 for SSP3-7.0 with pre-downscaling bias correction down to 9-km
    a. historical from 1980-2014
    b. SSP3-7.0 from 2015-2100

7. EC-Earth3-Veg for SSP3-7.0 with pre-downscaling bias correction down to 3-km for California and Wyoming grids
    a. historical from 1980-2014
    b. SSP3-7.0 from 2015-2100
8. FGOALS-g3 for SSP3-7.0 with pre-downscaling bias correction down to 9-km
    a. historical from 1980-2014
    b. SSP3-7.0 from 2015-2100

We note that the CESM2 non-SSP3-7.0 experiments share a common downscaled historical period (1980-2014). The additional simulations may be of interest to IOUs and climate researchers which is why they are mentioned here.

## 3. Data uses within EPC-20-006 and beyond

For EPC-20-006, WRF results will be used in different ways by the LOCA and hydrologic modeling teams. We emphasize that **dynamically downscaled data as part of Task 4 and presented above are not bias corrected in any way following downscaling**. However, select downscaled WRF variables will be bias corrected before ingestion into LOCA (Task 5). The WRF data will also be used by the hydrologic modeling team to produce streamflow projections (Task 6). As described in the section 4, below, the WRF data are subdivided into 3 tiers which can be used for various purposes. The hourly data can be used to create hourly climatologies and serve as input for land surface models, for example. The daily post-processed data are lightweight and can be easily used in geospatial physical analysis. Finally, the 6-hourly data can be used for more intensive analyses using the complete set of outputs from WRF, and the data can be used to create boundary conditions for even higher-resolution WRF experiments (beyond 3-km resolution).

## 4. Impacts of pre-downscaling bias correction

Although bias correction of the GCM simulations prior to WRF downscaling (i.e., a priori) was not used in EPC-20-006, the effects of a priori bias correction on the dynamical downscaled data is an open research question. Below we provide some preliminary evaluation of a priori bias correction of GCMs versus not. Figure 3 shows the vertical profile of GCM wintertime mean historical (1980-2014) biases in temperature and zonal wind relative to ERA5 across the eastern Pacific and western North America (20°-55°N and 140°-90°W mean). A tropospheric cold bias, a low-level instability bias, and a strong vertical shear bias are prevalent in the CMIP6 ensemble mean (30 GCMs, thick black curves). These three types of biases favor enhanced precipitation. When these mean-state biases are removed, we see significant drying of WRF's dynamically downscaled solution on the 9-km grid at SNOTEL locations across California's Sierra Nevada, both in terms of precipitation and snow water equivalent (Figure 4). Ultimately, the decision to not a priori bias correct the GCMs for EPC-20-006 was made because there was not sufficient time and computational resources to evaluate what uncertainty the bias correction may add to the finalized high-resolution product.

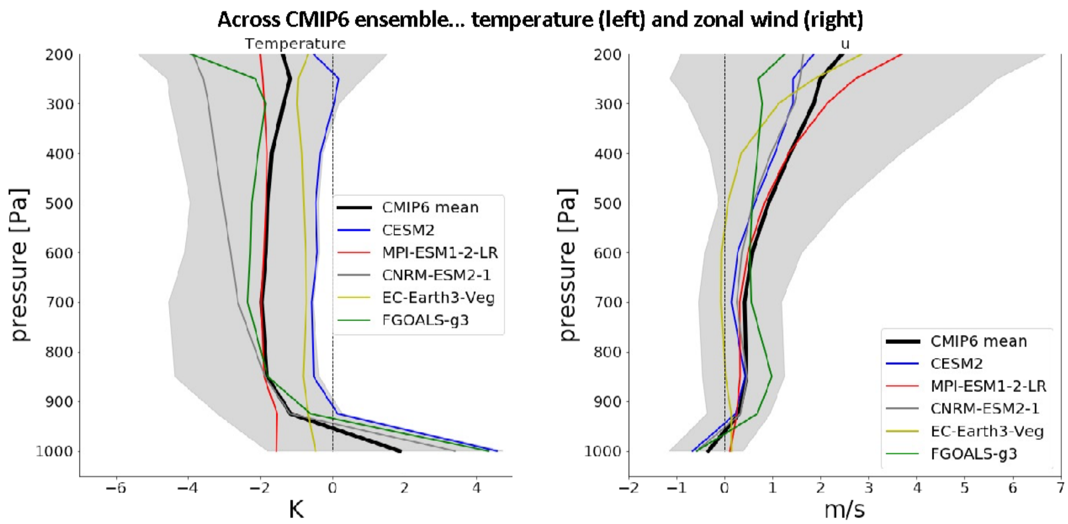


*Figure 3. Vertical profiles of historical (1980-2014) GCM mean-state biases in (left) temperature and (right) zonal wind averaged over 20°-55°N and 140°-90°W. The gray shading shows the spread from 30 CMIP6 GCMs, while the thick black curve denotes the bias in the ensemble mean. Colored curves are for 5 of our CMIP6 Historical simulations.*

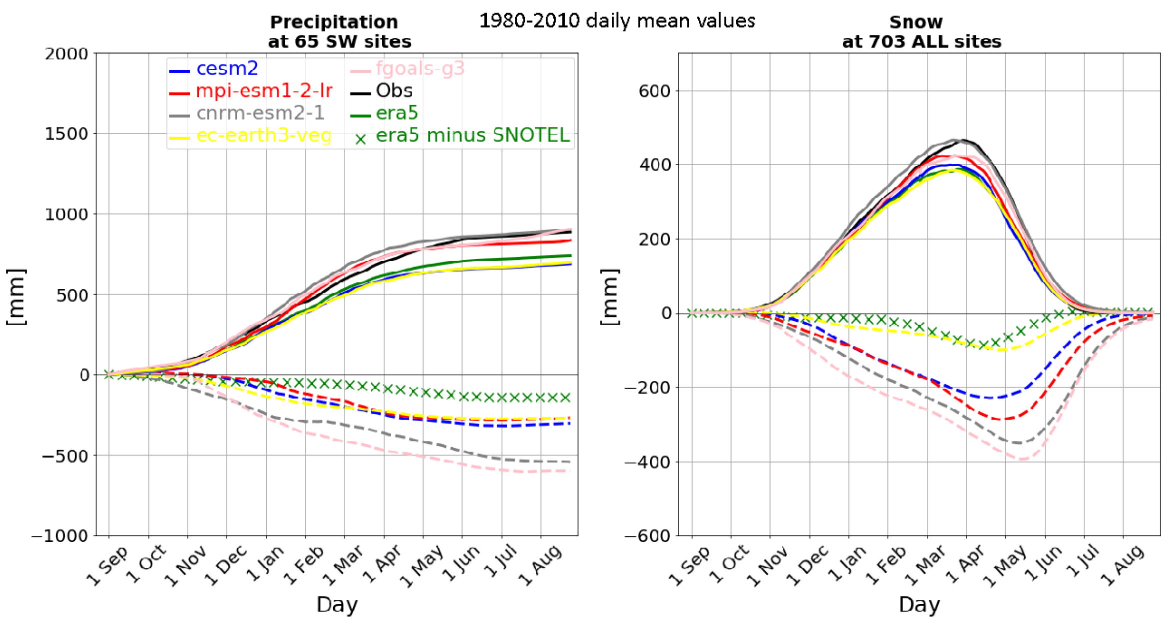


*Figure 4. Historical (1980-2010) site mean (left) cumulative precipitation and (right) snow water equivalent in mm from various bias corrected downscaled products on the 9-km grid (solid lines). Dashed curves show the difference between the bias corrected and non-bias corrected time series; negative values indicate a wetter solution in the non-bias corrected experiment. Green hatches show the differences between the ERA5-driven WRF experiment and SNOTEL observations; negative values indicate a wet bias in WRF.*

## 5. Access

All data discussed above is located in an open data bucket on Amazon S3. See bucket details at https://registry.opendata.aws/wrf-cmip6/. Amazon provides open-source software that allows for free and fast data transfers from S3 to your local devices via the Amazon Web Service Command Line Interface (AWS CLI). Specifically, all WRF data can be accessed on SE at:

1. **ERA5 downscaled reanalysi** – s3://wrf-cmip6-noversioning/downscaled_products/reanalysis/era5/
2. **CESM2 downscaled GCM** – s3://wrf-cmip6-noversioning/downscaled_products/gcm/cesm2_r11i1p1f1_historical/ *and* s3://wrf-cmip6-noversioning/downscaled_products/gcm/cesm2_r11i1p1f1_ssp370/
3. **CNRM-ESM2-1 downscaled GCM** – s3://wrf-cmip6-noversioning/downscaled_products/gcm/cnrm-esm2-1_r1i1p1f2_historical/ *and* s3://wrf-cmip6- noversioning/downscaled_products/gcm/cnrm-esm2-1_r1i1p1f2_ssp370/
4. **EC-Earth3-Veg downscaled GCM** – s3://wrf-cmip6-noversioning/downscaled_products/gcm/ec-earth3-veg_r1i1p1f1_historical/ *and* s3://wrf-cmip6- noversioning/downscaled_products/gcm/ec-earth3-veg_r1i1p1f1_ssp370/
5. **FGOALS-g3 downscaled GCM** – s3://wrf-cmip6-noversioning/downscaled_products/gcm/fgoals-g3_r1i1p1f1_historical/ *and* s3://wrf-cmip6- noversioning/downscaled_products/gcm/fgoals-g3_r1i1p1f1_ssp370/

## 6. References


Bruyère, C. L., Done, J. M., Holland, G. J., & Fredrick, S. (2014). Bias corrections of global models for regional climate simulations of high-impact weather. *Climate Dynamics*, *43*(7), 1847–1856. https://doi.org/10.1007/s00382-013-2011-6

Hersbach, H., Bell, B., Berrisford, P., Hirahara, S., Horányi, A., Muñoz-Sabater, J., et al. (2020). The ERA5 global reanalysis. *Quarterly Journal of the Royal Meteorological Society*, *146*(730), 1999–2049. https://doi.org/10.1002/qj.3803

Krantz,W., Pierce, D., Goldenson, N., Cayan, D. (2021) *Evaluation of CMIP6 GCMS Relevant for California Report* delivered to the CEC as result of Task 3 of EPC-20-006.

Mesinger, F., DiMego, G., Kalnay, E., Mitchell, K., Shafran, P. C., Ebisuzaki, W., et al. (2006). North American Regional Reanalysis. *Bulletin of the American Meteorological Society*, *87*(3), 343–360. https://doi.org/10.1175/BAMS-87-3-343

Rahimi, S., Krantz, W., Lin, Y.-H., Bass, B., Goldenson, N., Hall, A., et al. (2022). Evaluation of a Reanalysis-Driven Configuration of WRF4 Over the Western United States From 1980 to 2020. *Journal of Geophysical Research: Atmospheres*, *127*(4), e2021JD035699. https://doi.org/10.1029/2021JD035699

Skamarock, C., Klemp, B., Dudhia, J., Gill, O., Liu, Z., Berner, J., et al. (2019). A Description of the Advanced Research WRF Model Version 4. https://doi.org/10.5065/1dfh-6p97